NANO LETTERS

2007
Vol. 7, No. 6
1809−1816

Bifunctional Nanotube Scaffolds for Diverse Ligands Are Purified Simply from *Escherichia coli* Strains Coexpressing Two Functionalized Flagellar Genes

Richard D. Woods,[†] Noriko Takahashi,[‡] Akhmed Aslam,[†] Richard J. Pleass,[†] Shin-Ichi Aizawa,[‡] and R. Elizabeth Sockett*,[†]

Institute of Genetics, School of Biology, University of Nottingham, Queen's Medical Centre, Nottingham NG7 2UH, U.K., and CREST "Soft Nano-Machine Project", Innovation Plaza Hiroshima, 10-23 Kagamiyama, Higashi-Hiroshima 739-0046, Japan

Received February 6, 2007; Revised Manuscript Received April 13, 2007

ABSTRACT

We functionalized *Escherichia coli* FliC flagellin proteins to form tailored nanotubes binding single types or pairs of ligands, including divalent cations, fluorescent antibodies, or biotin-avidin-linked moieties such as ferritins. The ratio of each tag in bifunctionalized flagella could be toggled extending their sophistication as nanoscaffolds. Tobacco Etch Virus (TEV) protease site-containing FliCs were cleaved by the cognate protease without filament disintegration, potentiating their use as removable nanolithography masks to deposit attached ligands by protease cleavage.

As the field of nanotechnology develops, inspiration is drawn from nature, with the evolution in biological systems of self-assembling nanostructures through millions of years of molecular selection.[1] The building blocks of living organisms provide valuable miniature tools, as with proteins, attractive due to the complex, reproducible structures formed with nanoscale dimensions. With the progress made in genetic engineering, along with the advances in amino acid chemistry, biomolecules have been exploited to develop novel functional materials.[2−4] The assembly and use of biological nanotubes, as an alternative to carbon nanotubes, has been widely studied with diverse structures available.[5] Examples include harnessing the natural binding properties of pili[6] and virus-based magnetic and semiconducting nanowires.[7]

The bacterial flagellum is an impressive example of a self-assembling nanostructure, with more than 30 different proteins combining to form a 50 nm wide membrane-bound motor, a universal joint (hook), and long, thin filament which is rotated to act as a propeller.[8,9] The flagellar filament is a polymer of over 20 000 identical protein subunits, assembled into a helical hollow tube, with a diameter of 12−25 nm and central pore of only about 2−3 nm.[10] The single gene encoding these flagellin monomers can be easily engineered to allow the surface display of inserted epitopes along the length of the filament, creating a functional protein nanotube. The flagellin monomer has conserved regions at the N- and C-termini, required for anchoring the monomers into the filament structure.[8,10] However, the central region is variable and partially displayed on the filament surface. Significant portions of this variable region have been deleted and are shown to still produce assembled functional flagellar filaments.[11] Determination of the atomic structure of the flagellar filament in *Salmonella typhimurium* has allowed more detailed structural predictions to be made regarding which peptide sequences are fully displayed.[10]

As the structures of both the flagellar filament and the FliC monomer were elucidated, the potential for surface display along the length of the flagella was explored,[12] with antigen presentation research in *Escherichia coli*[13] and *Salmonella*.[14,15] Flagellin has been used to display a variety of adhesive peptides[16,17] and flagellin−thioredoxin fusions have been used to display conformationally constrained inserts as part of a disulfide loop.[18−20] More recently flagellar filaments have been constructed to display epitopes that are useful for vaccine developments.[17,21] Other uses for the flagella system have also been investigated, with the export apparatus harnessed to secrete heterologous recombinant proteins.[22]

* Corresponding author. E-mail: liz.sockett@nottingham.ac.uk. Telephone: 44-115 8230325.
[†] Institute of Genetics, School of Biology, University of Nottingham, Queen's Medical Centre.
[‡] CREST "Soft NanoMachine Project", Innovation Plaza Hiroshima.

10.1021/nl0702968 CCC: $37.00
Published on Web 05/10/2007

Here, we engineered flagellar filaments with functionalized surfaces that can be applied as useful alternatives to carbon nanotubes. Our idea is complementary to that of Kumara and co-workers[20] who produced cysteine-containing FliTrx proteins to form bundles of functionalized flagella but in our approach the functionalized FliCs can accept ligands or pairs of ligands, or can be cleaved specifically to deposit bound ligands on surfaces. This produces flagellar nanoscaffolds with a sophisticated range of potential applications. We also microscopically verified that the recombinant flagella produced were of micrometer lengths and we imaged the distribution of epitopes on their surfaces. Surface functionalization of chemically derived carbon nanotubes is possible, although reliability and reproducibility pose problems.[23] Genetic manipulation of flagellins allows tailoring of surface properties, which are homogeneous, in contrast to that seen with carbon nanotube functionalization. The functionalizing tags we tested were a poly histidine tag (HisFliC) to allow the binding of ligands via divalent cations including nickel and cobalt; a commercial avidin tag AviTag, which binds biotin (BioFliC) during synthesis, and allows binding of many other ligands via further avidin moieties, and a TEV− protease site tag (TEVFliC) which allows the site-specific cleavage of flagellin monomers upon addition of TEV protease. The precise assembly of the flagellar filaments means identical display of each functionalized monomer. With 11 flagellins per two turns of the filaments helical structure, for a filament of 1 μm length, 2200 identical peptide inserts can be displayed. Alternatively, by titrating the expression of two different flagellin genes, mosaic nanotubes with different percentages of dual functions can be produced. We have also characterized the efficiency of functionalized flagellar expression on bacterial cell surfaces and the motility properties of the strains with engineered flagella.

Strain Construction. Motile *E. coli* strain RP437[24] was used for construction of all strains expressing the functionalized *fliC*s, while strain DH5α was used for cloning purposes. Bacteria were grown with shaking in Mu broth (10 g/L tryptone, 5 g/L yeast extract, 10 g/L NaCl pH 7) for 16 h at 29 °C for maximal flagellar expression for motility-dependent experiments or at 37 °C for cloning. Media were supplemented with ampicillin 50 μg/mL, kanamycin 50 μg/mL, or chloramphenicol 25 μg/mL, when appropriate. Standard recombinant DNA techniques were used. Unless otherwise stated all chemicals were purchased from Sigma-Aldrich and restriction enzymes purchased from New England Biolabs or Invitrogen, and were used according to manufacturer's instructions. All primers were synthesized, and all sequencing was performed by MWG Biotech.

A *Bst*BI restriction site was engineered into the *fliC* gene of *E. coli* RP437, using overlap extension PCR with internal mutagenic primers *fliC*-*Bst*BI_F 5′-GGT GAT AAC GAT TTCGAA TAT TAC GC-3′ and *fliC*-*Bst*BI_R 5′-GCA ACT GTT ACT GCG TAA TATTCGAAA TCG TTA TCA CC-3′ (*Bst*BI site underlined) and end primers *fliC*_F 5′-CCC AAGCTT GGA CGC TGA TGG TGT ATT TCC-3′ and *fliC*_R 5′-GGAATT CCT TAA TCG GAC GAT TAG TGG G-3′ (introduced *Hind*III and *Eco*RI restriction sites underlined). Following PCR, the fragment was digested and ligated into the pUC19 cloning vector. This engineered *Bst*BI site allowed the in-frame insertion of DNA encoding "functionalizing" protein epitopes to be displayed on the surface of the flagella, between Asp^{242} and Tyr^{245}. The rationale used was that the site chosen should be unique within the DNA sequence of the *fliC* gene and allow, by mapping onto the *Salmonella* FliC structure, exposure of the functionalizing epitopes at the tip of the D3 domain of FliC. A 10× His-tag was designed with *Bst*BI ends (underlined) by annealing: His_F 5′- CGAACA TCA TCA CCA TCA CCA CCA TCA TCA CCA TAA GCT TTT-3′ and His_R 5′-CGAAAA GCT TAT GGT GAT GAT GGT GGT GAT GGT GAT GAT GTT-3′ and ligated into the engineered *Bst*BI site in *fliC*. The His-tagged *fliC* was ligated into the temperature sensitive suicide vector pST76-C to allow integration into the genome of *E. coli* RP437, as described in.[25,26] This procedure was repeated to create recombinant *fliC* strains containing a biotinylation site (AviTag - Avidity, Colorado[27,28]) and TEV protease site (2× to maintain similar length to other tags). For the Biotin tag the following oligonucleotides were used: Bio_F 5′ CGAAGG CCT GAA CGA CAT CTT CGA GGC TCA GAA AAT CGA ATG GCA CGA ATT 3′; Bio_R 5′CGAATT CGT GCC ATT CGA TTT TCT GAG CCT CGA AGA TGT CGT TCA GGC CTT 3′. For the TEV protease site the following oligonucleotides were used: TEV_F 5′ CGAAGA AAA CCT GTA TTT CCA GGG CGA AAA CCT GTA TTT CCA GGG CTT 3′; TEV_R 5′ CGAAGC CCT GGA AAT ACA GGT TTT CGC CCT GGA AAT ACA GGT TTT CTT 3′.

Characterization and Flagella Isolation. Two different methods were employed to isolate flagella from each recombinant or wild type strain. A vortex mixer was used to prepare low concentration, relatively crude flagella,[29] while a kitchen hand-blender (Braun MR4000) and centrifugation were used to prepare flagella of a higher concentration and purity. For the vortex preparations, 50 mL of overnight culture (OD_{600} nm >1.8) was pelleted (15 min, 5000*g*, +4 °C) and resuspended in 500 μL of 10 mM Tris, 0.1 mM EDTA pH 7.5 (TE), before vortexing in a microfuge tube (30 s, full power Fisons WM/250/F Whirlimixer). After pelleting of the bacteria (10 min, 13 000*g*, +4 °C) the flagella-containing supernatant was removed and stored at +4 °C. The blender method used 1 L of overnight culture pelleted by gentle centrifugation (30 min, 1328*g*, +4 °C) and gently resuspended in 100 mL of 10 mM HEPES pH 7 before shearing using the Braun MR4000 hand-blender (30 s, full power). The sheared bacteria from which filaments had been removed were pelleted (20 min, 15 000*g*, +4 °C) and discarded. The filament containing supernatant was centrifuged (90 min, 160 000*g*, +4 °C) to pellet the flagella, which were then resuspended in 300 μL of TE for ligand binding and electron microscopic analysis. Transmission electron microscopy (TEM) was used to image the both the recombinant bacteria and the sheared filaments on Formvar/Carbon 200 mesh Cu EM grids (Agar Scientific). The

samples were negatively stained with 1% or 2% phosphotungstic acid (pH 7).

Filament Decoration. His-tagged filaments were labeled using a monoclonal anti-poly-Histidine antibody produced in mouse (Sigma-Aldrich) and detected on blots using Western Breeze chemilumescent detection kit (Invitrogen). Fluorescent labeling of His-tagged filaments for visualization of cells and for FACS was carried out using a FITC-conjugated anti-mouse secondary antibody (Sigma-Aldrich). Immunogold labeling of His-tagged filaments for electron microscopy was carried out using a 5 nm gold particle-conjugated anti-mouse secondary antibody (Agar Scientific and Sigma Aldrich) as described in.[30] FACS analysis was carried out as follows. Equivalent volumes of RP437 and HisFliC cultures, matched by OD at 600 nm, were harvested by low-speed centrifugation (10 000*g*), resuspended gently (to minimize flagellar shearing) and washed twice in phosphate buffered saline (PBS; Invitrogen) supplemented with 0.5% BSA (PBA), followed by centrifugation, as described above. After blocking in 3% PBA for 30 min at room temperature, cells were incubated with primary antibodies diluted in 0.5% PBA (monoclonal anti-His, 1:1000; mouse IgG2a isotype control, 1:1000; or unstained buffer control) for 45 min at room temperature. Following further washes in PBA, cells were incubated with anti-mouse FITC-conjugated secondary antibody (Sigma-Aldrich) for 45 min. After the final wash stage, cells were resuspended in 0.5% paraformaldehyde and incubated in the dark at 4 °C. Fluorescence was measured by FACS analysis using an EPICS Altra flow cytometry system (Beckman Coulter, U.K.).

Constructing Chimeric Bifunctionalized Filaments. To test whether mosaic flagellar filaments could be produced expressing a combination of two functionalized FliCs, the expression vector pTRC99A[31] or a kanamycin-resistant derivative, pTRC99K, was used to construct and express pTRC99A_{fliC}, pTRC99K_{His}, pTRC99A_{TEV} and pTRC99A_{Bio}. The *fliC* genes were amplified from the respective *E. coli* strains using the primers pTRC_F CGAACCATGGCACAAGTCATTAATACC and pTRC_R CAGTTAATCAGTCGACAACGATTAACCC (*Nco*I and *Sal*I restriction sites underlined respectively). The *fliC* gene was then ligated in frame into pTRC99A using the *Nco*I and *Sal*I sites engineered into the PCR primers and the resulting vector transformed into the *E. coli* strains expressing tagged *fliC* genes. Induction of the *trc* promoter with varying concentrations of IPTG (0−500 μM) allowed differing expression levels of two different FliC monomers within the same bacterial cell. The integrity of genomic and plasmid copies of recombinant *fliCs* were confirmed by PCR, DNA sequencing, and SDS−PAGE analysis. Changes in motile phenotype were confirmed by light and electron microscopy, and inoculation in 0.35% agar swarm plates which allow the swimming of motile cells to form swarms.

Monitoring Expression of Functionalized Flagella and Effects on Cell Motility. All engineered strains produced flagellar filaments that could be readily sheared from cells by simple blender or vortex treatment and could be visualized on SDS−PAGE. The functionalized FliCs ran with different apparent molecular weights: RP437 55 kDa, HisFliC 63 kDa, TEVFliC 67 kDa, and BioFliC 69 kDa. This was caused by the diverse inserted tags, due to a combination of charge and amino-acid mass differences (and biotin or metal binding for BioFliC or HisFliC); this was a convenient way to differentiate functionalized FliCs from each other. (Figure 1a,c). Harvested yields of recombinant flagellin proteins were found to be approximately 40 times less than that of wild type RP437 FliC when vortex treatments were used but only 5 times less when using the blender method. Flagella were expressed as fully formed filaments on the surfaces of each strain although they were shorter and less numerous than those on wild type RP437 **(**Figure 1b**)**. Interestingly, the nature of the tag affected flagellar motility as seen by phase contrast microscopy of wet mounts of cultures, where percentage motility of populations of all tagged strains was much lower than wild type RP437. Cells of the recombinant strain encoding chromosomally the His tagged FliC were seen in tangled clumps writhing against each other (Figure 1b). Motility analysis of the cultures on 0.35% agar swarm plates (1% tryptone, 0.5% NaCl) showed that for the HisFliC strain the tangling of the flagella was sufficient to prevent outward swimming motility of the culture, despite the good number of flagellar filaments on the surface (Figure 1d). For the BioFliC and TEVFliC strains the size of the motile swarms was reduced to half of wild type. As evolution has shaped flagellar filament surfaces, over millions of years, to be monomers that are readily transportable up the hollow center of the growing flagellum and to produce nontangling smooth propellers; it is not surprising that shorter and fewer filaments that tangle are made in the recombinant strains where foreign amino-acid tags have been introduced to the FliC surfaces (Figure 1). For the HisFliC strain it is likely that the co-ordinate binding, between filaments of endogenous metal ions in the bacterial growth medium or swarm plate medium, causes the excessive cell clumping, and lack of motility seen. However, this did not adversely affect the harvesting of flagellar filaments from the cell surface by shearing.

The functionalizing tags were predicted to be exposed on the surface of the *E.coli* flagellin proteins (Figure 1e) and this was confirmed experimentally for each flagellin type. The presence of the biotin bound to the avidity tag in BioFliC strains was revealed by the binding of ferritin-avidin nanoparticles (A5405 Sigma-Aldrich). The presence of the TEV protease site in TEVFliC strains was determined by digestion with AcTEV protease (Invitrogen) using standard conditions overnight at 4 °C. That the 10× His-tag was displayed on the surface of HisFliC cells was confirmed by both Western blotting with an anti-His monoclonal antibody **(**Figure 2a) and by binding of diverse metal nanoparticles (data not shown). Fluorescent microscopy with primary anti-His and FITC-conjugated secondary antibodies revealed fluorescent foci corresponding to groups of flagella on the cell surface (Figure 2b). The expression of His-tagged flagellar filaments on HisFliC cells was also confirmed using flow cytometry. Over 50% of the HisFliC cells displayed significant fluo-

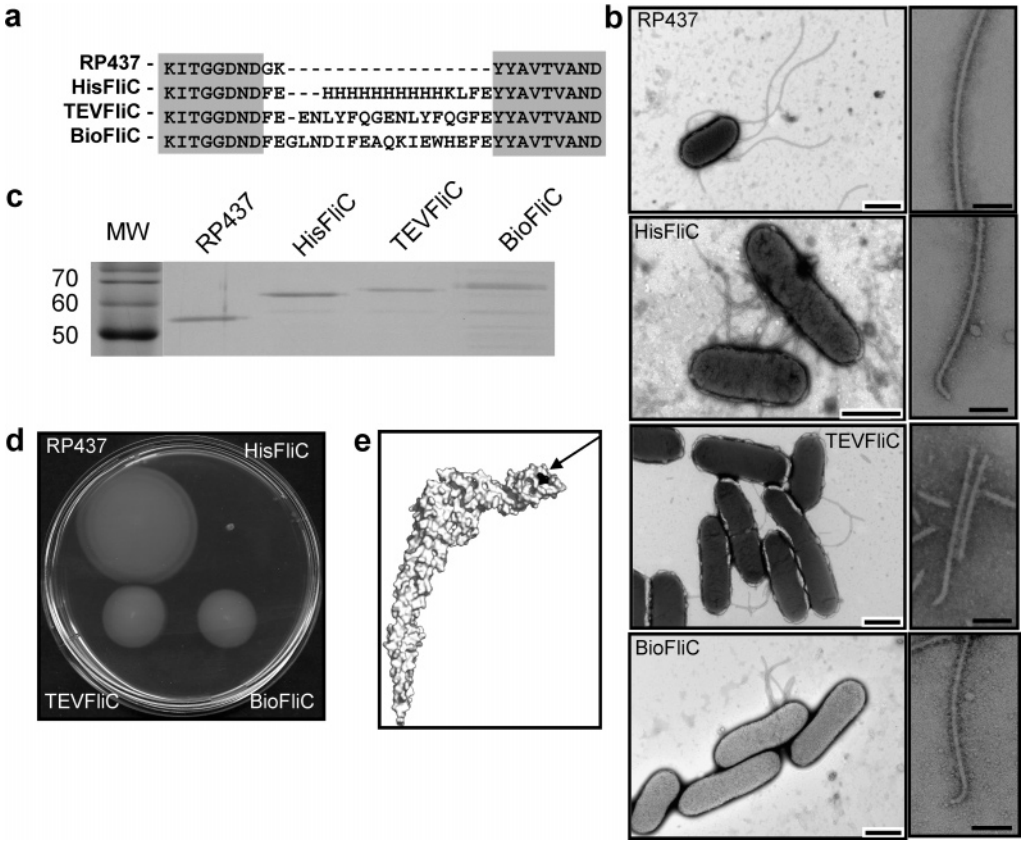

Figure 1. Flagellar filament formation and motility in wild type and functionalized *fliC* strains of *E. coli* RP437. (a) Amino-acid inserts into the wild type (RP437) sequence to give functionalized His, TEV and Bio FliC proteins. (b) SDS−PAGE [12%] of filaments vortex-prepared from matched OD_{600nm} cultures with chromosomally engineered *fliC* genes expressing the single tag sequences indicated above each lane. 20 μL of each FliC preparation was loaded per lane except for wild type RP437 where 20 μL of a 1/40th dilution of sample was used. (c) Negatively stained transmission electron micrographs (TEMs) of cells and isolated functionalized filaments for each strain (scale bars 1000 nm for cells, 100 nm for filaments). (d) Soft agar swarm plate assay of motility of the three recombinant strains, after 14 h incubation at 29 °C, compared to wild type RP437. (e) Model of RP437 FliC protein sequence mapped onto the atomic structure of Salmonella flagellin (PDB 1UCU) using the 3D-JIGSAW Protein Comparative Modeling Server,[38] on which the predicted tag insertion site is highlighted in black.

rescence above wild type RP437 cells (mean fluorescent intensity of 19.82 and 4.18, respectively) using FACS analysis, indicating that this number of cells were expressing the filaments. The lack of isotype control antibody-binding to HisFliC filaments showed that the FITC fluorescence observed was only due to anti-His positive binding to flagella (Figure 2c), and confirmed our observations by microscopy. Purified HisFliC filaments could be regularly decorated along their length with 5 nm immunogold conjugated secondary antibodies, revealing the His tags to be accessible for ligand binding on the functionalized flagellar surface (Figure 2d). Similarly, the BioFliC filaments could be decorated, on EM grids, with avidin conjugated to 8−12 nm horse-spleen ferritin nanoparticles (Figure 2e). This interesting result showed that the AviTag introduced into the FliC monomer sequences was being biotinylated inside the *E. coli* cells, presumably by the endogenous *birA* gene; prior to the export of the BioFliC monomers up the hollow center of the growing flagellum. Thus, the biotin attached to the AviTag was no impediment to recognition of the FliC protein by the Type III flagellar export apparatus nor was it an impediment to conductance of the monomers up the flagellar core.[9]

That the TEV protease site was cleavable on the surface of the TEVFliC filaments, to give two approximately 30 kDa products, without further degradation of the flagellin protein and that wild type RP437 FliC filaments were not cleaved, was shown by SDS−PAGE (Figure 2f), but TEVFliC filaments were still seen to be intact by TEM (Figure 2g). This was expected because the conserved N- and C-terminal ends of FliC monomers comprise the binding sites that make up the polymerized filament. Cleavable TEV sites positioned either side of another functionalizing tag would allow functionalized flagella to become nanoscale printing/lithography masks. These would deposit nanoligands, such as metals loaded onto HisFliC filaments (with the His flanked by TEV tags) in a regular pattern dictated by the (nm × μm) dimensions of the functionalized FliC filament, along a surface with the cleaved flagellar filament "mask" being washed off following TEV cleavage.

Having established that flagella could be surface-functionalized as nanotubes with a single type of epitope tag, we used IPTG-induced expression of *fliCs* from pTRC99A or pTRC99K in the different single functionalized *fliC* chromosomally engineered strains to ask whether we could synthesize mixed flagellar nanotubes with two different tags

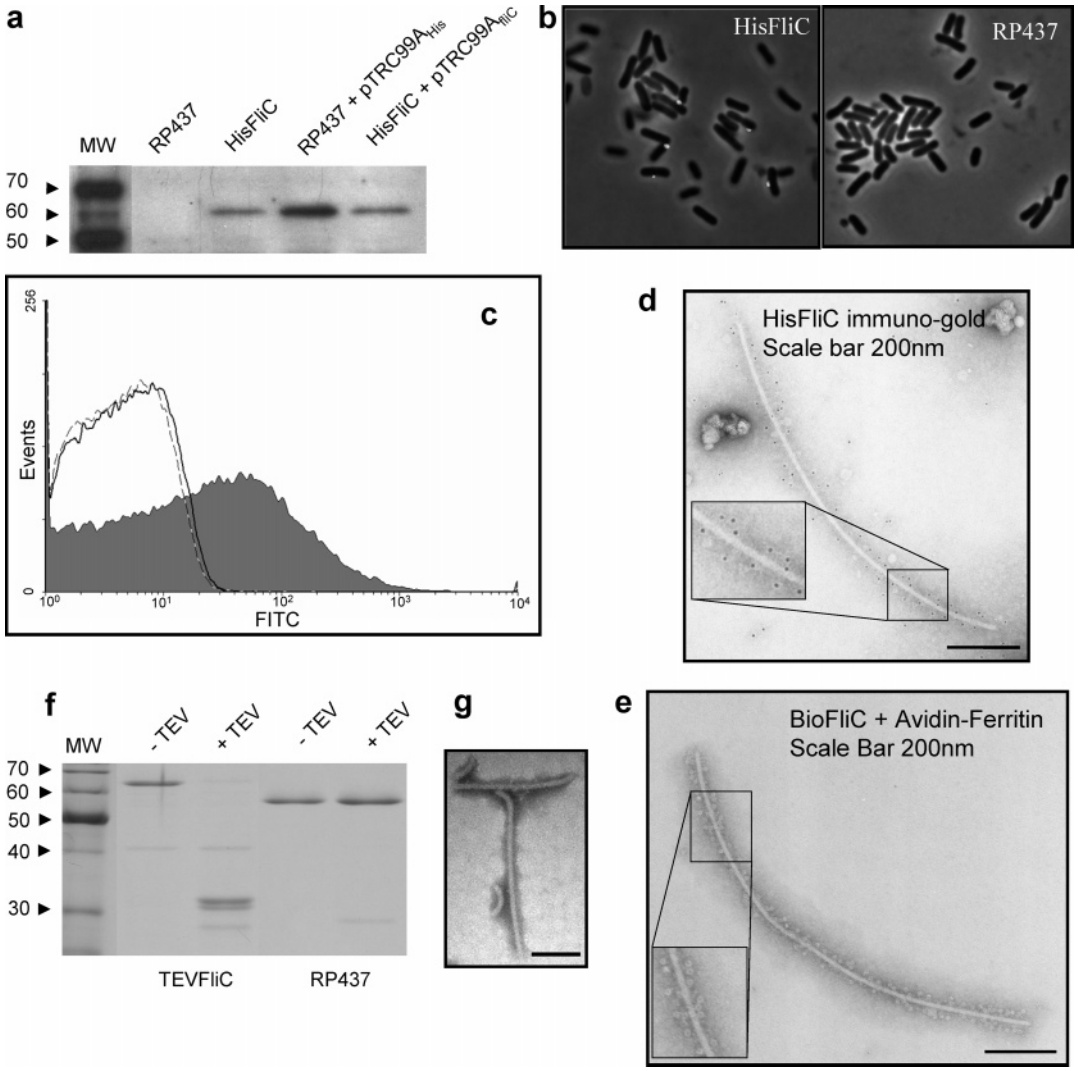

Figure 2. Detection and quantification of ligand-binding on the surfaces of functionalized flagella. (a) Western blot with anti-His monoclonal antiserum detects HisFliC band of 63 kDa molecular weight in matched OD_{600nm} whole cell extracts of chromosomally engineered HisFliC strain and wild type RP437 strain expressing HisFliC from plasmid pTRC99A, but not wild type RP437 strain alone. (b) Fluorescence microscopy of FITC secondary antibody detection of the monoclonal anti-His binding to the outside of cells from cultures of HisFliC vs RP437 wild type. (c) FACS analysis showing FITC fluorescence for anti-His binding to surface flagella on the HisFliC (filled gray area) or RP437 (bold line) strains vs Isotype control antibody (dashed line) -which was ineffective at binding to HisFliC cells. (d) TEM of 5 nm immunogold-secondary-antibody, binding to HisFliC filaments. (e) TEM for the BioFliC filaments avidin-conjugated 8−12 nm horse spleen ferritin particles decorated the length of the filaments. (f) SDS−PAGE analysis of protease treatment of TEVFliC and RP437 filaments, showing digest patterns produced when 5 μg of filament protein was loaded in each lane, after treatment of 25 μg of each filament type with or without (±) 10U of AcTEV protease (seen itself as a 29 kDa band). (g) Negatively stained electron micrograph of TEVFliC filaments following TEV treatment for 12 h at 4 °C, showing that the filaments are substantially intact (scale bar 100 nm).

in one mosaic filament. Pairwise combinations were tried for all three functionalized FliCs and for wild type RP437; typical data are shown for the HisFliC strain transformed with the plasmid pTRC99A$_{Bio}$ or for the reverse BioFliC strain transformed with a plasmid incorporating the His tag (pTRC99K$_{His}$) combination. In both cases, taking the HisFliC: pTRC99A$_{Bio}$ combination as an example, induction with IPTG caused a decrease in the proportion of chromosomally encoded FliC protein appearing in purified, sheared filaments, as the proportion of plasmid encoded filament rose with increasing IPTG concentration (Figure 3a). Thus, there seems to be an upper threshold amount of FliC that can be produced in cells and it may be possible to "toggle" the amounts of each FliC type in the total produced, by varying IPTG levels. That the different expression of BioFliC and HisFliC affected the nature of the flagellar filaments produced and the motility of the cultures expressing the other functionalized FliC chromosomally, was evident from swarm plates as expected (Figure 3b). Coexpression of the filament-tangling His-tagged FliC from pTRC99K$_{His}$ in the BioFliC strain reduced the strain swarm size and hence motility. Conversely, expression of the pTRC99A$_{Bio}$ in the HisFliC strain increased swarm diameter and motility of that strain. Labeling with avidin-ferritin and also with secondary 5 nm immuno−gold antibody detection of primary anti-His antibody in filaments sheared from such dual His/BioFliC-expressing strains showed definitively that both His and Bio FliCs were contained within the same mosaic filaments, as these were

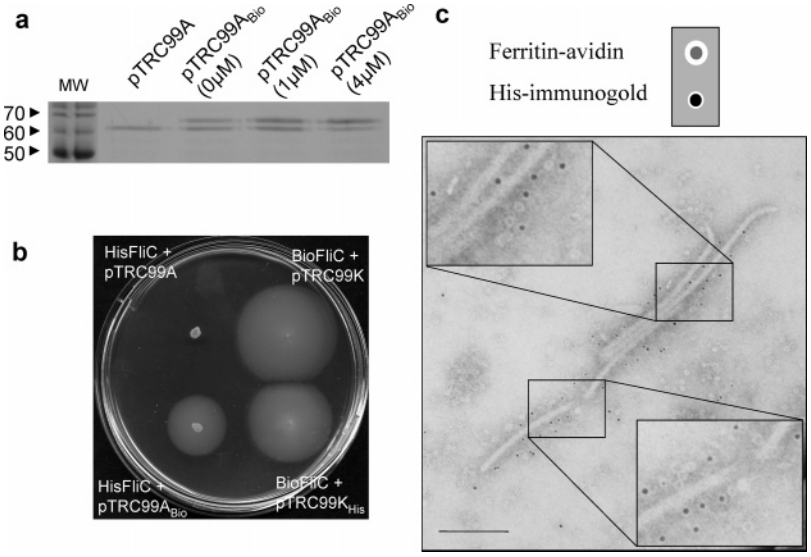

Figure 3. Coexpressing 2 functionalized FliCs to make bifunctional flagellar nanotubes. (a) SDS−PAGE [12%] of vortex preparations of sheared flagella from HisFliC cells expressing BioFliC from the vector pTRC99A$_{Bio}$ or empty vector control. Cultures were all matched to the same OD_{600nm}, prior to shearing. Different levels of IPTG induction are shown with the ratio of the upper BioFliC band increasing to dominate over the lower HisFliC band as IPTG concentrations are raised from 1 μM to 4 μM. (b) Soft agar swarm plate assay of motility, after 20 h incubation at 29 °C of both the BioFliC strain expressing an approximately equal amount of HisFliC due to 1 μM IPTG promoting HisFliC expression from pTRC99K$_{His}$ and the converse HisFliC strain expressing the BioFliC due to 1 μM IPTG promoting HisFliC expression from pTRC99A$_{Bio}$. (c) Mosaic filaments sheared from HisFliC strains expressing pTRC99A$_{Bio}$ due to 1 μM IPTG induction are decorated with *both* 5 nm immunogold conjugated secondary antibodies binding to anti-His primary antibodies that attach to HisFliC monomers *and* avidin-conjugated 8−12 nm horse spleen ferritin particles that bind to BioFliC monomers (scale bar 200 nm).

labeled by both particles simultaneously (Figure 3c). Proof that single HisFliC control filaments did not bind avidin-ferritin and that BioFliC control filaments did not bind anti-His was obtained (supporting online material Figure 1). Thus, mosaic functionalized flagella with dual binding properties can be simply synthesized for use in nanotechnology applications.

Discussion. Here we have shown that the insertion of functional tags between Asp[242] and Tyr[245] of the *E. coli* flagellin are surface-displayed on the flagellar filament tailoring it for nanoscaffold uses. A variety of small peptide tags have been expressed in this location, ranging from 16 amino acids in HisFliC to the 19 amino acids in BioFliC. All tags produced bacterial strains with altered swarm plate motility phenotypes and a degree of flagellar aggregation, likely due to the altered charges present on the surface of the flagella. This is not surprising considering evolution has shaped these appendages for the specific task of motility, over millions of years, and therefore eliminated any residues which may cause binding and impede motility. The HisFliC strain was seen to form the highest proportion of writhing, motile, flagellar-attached clumps in liquid culture, and had least directional motility on swarm plates, suggesting binding between filaments was strongest in this strain. Metal atoms from culture media are bound by the histidine residues (data not shown) with ligands to the metal atoms forming coordinate bonds between filaments. The TEVFliC and BioFliC strains do not contain extensive metal-binding amino acids but their tags do contain several polar glutamate residues and also hydrophobic residues that may enhance filament−filament binding interactions compared to the wild type (Figure 1a).

Shearing of the engineered filaments from the respective strains was possible using vortexing methods and by using a simple Braun domestic blender; each strain produced truncated filaments compared to the wild type, even though an identical protocol was used for each. This truncation may be due to the mechanical stresses involved in engineered filaments rotating while being tethered to other filaments or, possibly, due to the less efficient transportation of tagged FliC monomers up the hollow core of the growing flagellum compared to wild type. The structural weakness of these engineered filaments was to be expected as previous work has detailed the importance of the variable region in stabilizing the filament structure.[32−34] Even these small tag insertions into the variable region will have caused a degree of warping, leading to a reduction in stabilizing interactions. The filaments rarely exceeded 1 μm in length, although we were able to use in vitro polymerization with ammonium sulfate preparations of FliCs to produce nanotubes of increased length[35,36] (data not shown).

Immunofluorescence microscopy demonstrated that the 10x His-tag was surface displayed and could be recognized by antibodies in its native folded state. Immunogold labeled secondary antibodies were used to visualize the tags on the surface of the HisFliC filaments by TEM, demonstrating specific binding of immunogold particles. The flagellar filaments of the BioFliC strain bound avidin-conjugated horse spleen ferritin particles directly, and these were visualized as 8−12 nm particles with an electron dense metal center. This showed that the AviTags on the BioFliCs were being biotinylated *in vivo*, probably by biotin protein ligase naturally expressed in *E. coli*, yet biotinylation did not impede translocation of the FliCs up the center channel of

the growing flagellum to polymerize at the growing tip of the filament. Although high efficiency biotinylation seems evident here, this could be further increased by overexpression of the *birA* gene or by supplementing the growth media with biotin. Mass spectrometry could be used to quantify any increase in tag biotinylation. These biotinylated flagella facilitate the direct attachment of a variety of avidin-labeled ligands that may allow future nanotechnology applications, where tailored diverse avidin-linked nanostructures could be attached; or the filaments could be immobilized on avidin coated surfaces. This may allow flagellar filaments to be employed as structural bridges or links between components of an artifical nanomachine, to act as strands of insulation in nanocircuits, or if His or Bio FliC filaments were combined with metal-binding epitopes and metal nanoparticles, to possibly conduct current or act as small magnetic strands in nanomachines.

Insertion of the TEV protease tag allowed cleavage of TEVFliC within assembled filaments, at the variable, surface-exposed site. Digestion of the 67 kDa TEVFliC protein with TEV protease produced two bands of 31 kDa and 33 kDa in size, as seen by SDS−PAGE analysis. When imaged by TEM, TEV-treated flagellar filaments in this sample were still intact with no apparent structural change because, without denaturing treatment for SDS−PAGE, the monomers were still polymerized into filaments with the TEV sites on the outer exposed surface. Thus, the intermolecular bonds within the N- and C-termini of the flagellins were strong enough to maintain the integrity of the flagellar filament structure, even though the variable region had been nicked. This means that filaments could be attached to a surface, by an epitope tag, but have flanking TEV protease sites to allow swift removal of intact filaments at will. This facilitates the deposition of tags or their attached nanoligands in trails, mirroring flagellar filament dimensions: several micrometers long by multiples of 15 nm wide using the flagellar filaments as nanoscale masks.

Conclusion. The work reported here extends the use of bacterial flagella from the work of other pioneers for antigen display and epitope secretion[13,14,16,17] to their use as structural nanotubes and micrometer-scale, cleavable nanotemplates for laying down specific epitopes on surfaces. The strengths of our functionalized flagella, compared to conventionally labeled carbon-nanotubes, are that they homogeneously express their surface epitopes, can be simply purified and cheaply produced, and that two functionalized FliCs can be produced at varying concentrations in a single filament giving different degrees of mixed-nanoligand binding. The AviTag avidin−biotin moiety allows extensive ligation of other nanostructures to build up networks and the accessible and specific TEV protease cleavage site shows that such ligands can be released from the filaments if desired.

Note Added in Proof. While this manuscript was under review, Kumara and co-workers showed that His functionalized flagella could indeed be used as scaffolds for the binding of diverse metal nanoparticles.[37]

Acknowledgment. This work was funded by a Ph.D. studentship for R.D.W., from the Nottingham University Nanotechnology IDTC Programme and by BBSRC Flagellar toolkit Grant 42/P18196 to R.E.S. and by the CREST Soft Nanomachine project to S−IA. Collaboration between the R.E.S. and S.-I.A. labs is stimulated by HFSP Programme Grant RGP0057/2005. We thank Stephanie Allen, Saul Tendler, and the Nottingham Nanotechnology IDTC for the provision of part of the Ph.D. studentship to R.D.W. We thank Karen Morehouse, Carey Lambert, John Taylor, Mark Smith, and Jessie Wood for helpful discussions, Trevor Gray and Katy Evans for assistance with electron microscopy, and Laura Hobley and Ross le Grand for assistance with strains and culturing. Technical support in the laboratory is provided by Rob Till, Mike Capeness, and Marilyn Whitworth.

Supporting Information Available: Supplementary Figure 1, control images of BioFliC and HisFliC binding. This material is available free of charge via the Internet at http://pubs.acs.org.

References

(1) Seeman, N. C.; Belcher, A. M. *Proc. Natl. Acad. Sci. U.S.A.* **2002**, *99* (Suppl 2), 6451−6455.
(2) Katz, E.; Willner, I. *Angew. Chem. Int. Ed. Engl.* **2004**, *43*, 6042−6108.
(3) Wu, L. Q.; Payne, G. F. *Trends Biotechnol.* **2004**, *22*, 593−599.
(4) Zhang, S. *Biotechnol. Adv.* **2002**, *20*, 321−339.
(5) Bong, D. T.; Clark, T. D.; Granja, J. R.; Ghadiri, M. R. *Angew. Chem. Int. Ed. Engl.* **2001**, *40*, 988−1011.
(6) Reguera, G.; McCarthy, K. D.; Mehta, T.; Nicoll, J. S.; Tuominen, M. T.; Lovley, D. R. *Nature (London)* **2005**, *435* (7045), 1098−1101.
(7) Mao, C.; Solis, D. J.; Reiss, B. D.; Kottmann, S. T.; Sweeney, R. Y.; Hayhurst, A.; Georgiou, G.; Iverson, B.; Belcher, A. M. *Science* **2004**, *303* (5655), 213−217.
(8) Namba, K.; Vonderviszt, F. *Q. Rev. Biophys.* **1997**, *30* (1), 1−65.
(9) Macnab, R. M. *Annu. Rev. Microbiol.* **2003**, *57*, 77−100.
(10) Yonekura, K.; Maki-Yonekura, S.; Namba, K. *Nature (London)* **2003**, *424* (6949), 643−50.
(11) Kuwajima, G. *J. Bacteriol.* **1988**, *170*, 3305−3309.
(12) Fedorov, O. V.; Efimov, A. V. *Protein Eng.* **1990**, *3*, 411−413.
(13) Kuwajima, G.; Asaka, J.-I.; Fujiwara, T.; Nakano, K.; Kondoh, E. *Biotechnology (N.Y.)* **1988**, *6*, 1080−1083.
(14) Wu, J. Y.; Newton, S.; Judd, A.; Stocker, B.; Robinson, W. S. *Proc. Natl. Acad. Sci. U.S.A.* **1989**, *86*, 4726−4730.
(15) Newton, S. M.; Jacob, C. O.; Stocker, B. A. *Science* **1989**, *244* (4900), 70−72.
(16) Westerlund-Wikstrom, B.; Tanskanen, J.; Virkola, R.; Hacker, J.; Lindberg, M.; Skurnik, M.; Korhonen, T. K. *Protein Eng.* **1997**, *10*, 1319−1326.
(17) Tanskanen, J.; Korhonen, T. K.; Westerlund-Wikstrom, B. *Appl. Environ. Microbiol.* **2000**, *66*, 4152−4156.
(18) Lu, Z.; Murray, K. S.; Van, Cleave, V.; LaVallie, E. R.; Stahl, M. L.; McCoy, J. M. *Biotechnology (N.Y.)* **1995**, *13*, 366−372.
(19) Tripp, B. C.; Lu, Z.; Bourque, K.; Sookdeo, H.; McCoy, J. M. *Protein Eng.* **2001**, *14*, 367−377.
(20) Kumara, M. T.; Srividya, N.; Muralidharan, S.; Tripp, B. C. *Nano Lett.* **2006**, *6*, 2121−2129.
(21) Majander, K.; Korhonen, T. K.; Westerlund-Wikstrom, B. *Appl. Environ. Microbiol.* **2005**, *71*, 4263−4268.
(22) Majander, K.; Anton, L.; Antikainen, J.; Lang, H.; Brummer, M.; Korhonen, T. K.; Westerlund-Wikstrom, B. *Nat. Biotechnol.* **2005**, *23*, 475−481.
(23) Sinnott, S. B. *J. Nanosci. Nanotechnol.* **2002**, *2*, 113−123.
(24) Parkinson, J. S. H.; S. *J. Bacteriol.* **1982**, *151*, 106−113.
(25) Posfai, G.; Koob, M. D.; Kirkpatrick, H. A.; Blattner, F. R. *J. Bacteriol.* **1997**, *179*, 4426−4428.
(26) Posfai, G.; Kolisnychenko, V.; Bereczki, Z.; Blattner, F. R. *Nucleic Acids Res.* **1999**, *27*, 4409−4415.
(27) Schatz, P. J. *Biotechnology (N.Y.)* **1993**, *11*, 1138−1143.

(28) Beckett, D.; Kovaleva, E.; Schatz, P. J. *Protein Sci.* **1999**, *8*, 921−929.
(29) Trachtenberg, S.; DeRosier, D. J. *J. Bacteriol.* **1992**, *174*, 6198−6206.
(30) Ohnishi, K.; Ohto, Y.; Aizawa, S.; Macnab, R. M.; Iino, T. *J. Bacteriol.* **1994**, *176*, 2272−2281.
(31) Amann, E.; Ochs, B.; Abel, K. J. *Gene* **1988**, *69*, 301−315.
(32) Yoshioka, K.; Aizawa, S.; Yamaguchi, S. *J. Bacteriol.* **1995**, *177*, 1090−1093.
(33) Mimori-Kiyosue, Y.; Yamashita, I.; Fujiyoshi, Y.; Yamaguchi, S.; Namba, K. *J. Mol. Biol.* **1998**, *284*, 521−530.
(34) Samatey, F. A.; Imada, K.; Nagashima, S.; Vonderviszt, F.; Kumasaka, T.; Yamamoto, M.; Namba, K. *Nature (London)* **2001**, *410* (6826), 331−337.
(35) Ikeda, T.; Kamiya, R.; Yamaguchi, S. *J. Bacteriol.* **1984**, *159*, 787−789.
(36) Sherman, P.; Soni, R.; Yeger, H. *J. Clin. Microbiol.* **1988**, *26*, 1367−1372.
(37) Kumara, M. T.; et al. Self-Assembly of Metal Nanoparticles and Nanotubes on Bioengineered Flagella Scaffolds. *Chem. Mater.* **2007**, *19*, 2056−2064. Kumara, M. T.; et al. Exciton Energy Transfer in Self-Assembled Quantum Dots on Bioengineered Bacterial Flagella Nanotubes. *J. Phys. Chem. C.* **2007**, *111*, 5276−5280.
(38) 3D-JIGSAW Protein Comparative Modeling Server. http://www.bmm.icnet.uk/servers/3djigsaw/.

NL0702968